esa climate change initiative
European Space Agency

Option 3

Climate Change Impact Assessment (CCIA)

glaciers cci

Prepared by:	Glaciers_cci consortium
Contract:	4000101778/10/I-AM
Name:	Glaciers_cci-O3D4_CCIA
Version:	0.3
Date:	30.07. 2014

Contact:
Frank Paul
Department of Geography
University of Zurich
frank.paul@geo.uzh.ch

Technical Officer:
Stephen Plummer
ESA ESRIN

University of Zurich[UZH]

GAMMA

UNIVERSITY OF OSLO

Document status sheet

Version	Date	Changes	Approval
0.1	22.02. 2014	First draft	
0.2	28.06. 2014	All assessments integrated	
0.3	30.07. 2014	Comments from TO integrated	

The work described in this report was done under ESA contract 4000101778/10/I-AM. Responsibility for the contents resides with the authors that prepared it.

Author team:
Nico Mölg, Frank Paul, Tobias Bolch (GIUZ), Andreas Kääb, Christopher Nuth (GUIO), Tazio Strozzi (Gamma)

Glaciers_cci Technical Officer at ESA:
Stephen Plummer

Table of Contents

1. Introduction

This is deliverable 4 of Option 3 (O3D4) of the Glaciers_cci project, the climate change impact assessment (CCIA). The document illustrates first results of applications with the improved glacier outlines for regions in the Karakoram and Pamir. The datasets used to create the results are presented in deliverable 3, the glacier inventory data package (GIDP).

The quality-improved outlines allowed us to analyse how glaciers have changed over the past decades. We have selected the Karakoram region with its high number of frequently surging glaciers for this assessment (e.g. Bhambri et al. 2013, Copland et al. 2011, Hewitt 2007, Rankl et al. 2014). For this purpose we manually delineated glacier extents on satellite images from the 1970s based on Landsat MSS, and declassiefied Corona and Hexagon images. The latter two were quite difficult to georeference, so it was decided to only digitize terminus positions and derive a more qualitative glacier change index rather than (quantitative) area changes per glacier.

The direct comparison between our new and the previous outlines from the Randolph Glacier Inventory (RGI) 3.0 (shown in the GIDP) revealed only small overall changes in glacier area, but only a 72% overlap of both datasets. These omission and commission errors resulted in a wrong selection of ICESat footprints over glaciers for assessment of point elevation changes in previous studies by Kääb et al. (2012) and Gardner et al. (2013). We have thus re-analysed for this deliverable how the previously derived elevation changes differed from those derived for the new outlines. Further applications of the new dataset (e.g. a revised calculation of total glacier volume) are intended to be performed in Phase 2 of the CCI programme.

2. Area changes

2.1 Study Region and datasets

Starting from the key regions corrected for Option 3, we decided to prioritise regions with the largest glacier extents and uncertainties regarding our knowledge of glacier area changes during the last few decades. An additional role was played by the availability of comparable EO datasets in sufficient quality over larger regions. Based on this, we selected the Pamir-Fechenko region and the Central Karakoram around Siachen, Baltoro and Hispar glaciers.

We decided to use Landsat MSS and the now declassified Corona and Hexagon satellite data acquired between 1969 and 1980 for area change assessment, as they provide the largest temporal coverage with regard to our inventory from the year 2000. Additonally, the scenes had to fulfill the requirements for successful glacier mapping (in particular minimum extent of seasonal snow cover). We georeferenced and delineated glaciers on two Hexagon, three Corona and three Landsat MSS scenes. The image foorprints are shown in Fig. 15 of the GIDP, image quicklooks are shown in Figs. 16 to 18 of the GIDP and details are listed in Table 4 of the same document.

2.2 Methods

Georeferencing had to be performed for one MSS and all Hexagon and Corona scenes. For one of the two parts of the Hexagon scene a Python script of the TU Dresden has been used (cf. Pieczonka et al. 2013), but the processing chain had several difficulties and the ArcGIS warp tool used for the final geometric correction often failed. One half of the one Hexagon scene as well as the other scenes have therefore been rectified and georeferenced manually using the ERDAS Imagine 2011 “Project Transformation” tool. It takes as an input manually derived ground control points (GCP) and a DEM (here we used the ASTER GDEM II due to better quality compared to the SRTM DEM). The results are reasonably useful, but are locally strongly depending on the density of the GCPs and the quality of the DEM. Only the scenes with best quality have been treated, because the processing is very time consuming, Therefore the number of processed and analysed scenes were reduced to seven (see Table 4 in te GIDP). The MSS scenes were already orthorectified by USGS (to L1T) except one scene that was manually adjused to the geometry of the ETM+ scene.

Due to the partly unsatisfying geometric accuracy, the new outlines have been manually digitised with a focus on the region of the glacier terminus. To achieve a good comparison the master outlines derived in Option 3 from around the year 2000 were copied and adjusted at the glacier tongue with the orthorectified historic image in the background. A couple of screenshots for the same region is shown for the three sensors in Figs. 1 to 6. The procedure was constrained to a subsample of glaciers whose terminus could clearly be determined at both points in time. Only these are shown by outlines in the respective figures. This led to the investigation of 60 glaciers from 1969 to 2000 (Corona), 249 from 1972/76/77 to 2000 (MSS) and 84 from 1980 to 2000 (Hexagon). Altogether 251 different glaciers have been analysed. They are marked on the overview image depicted in Fig. 7. The analysis will be extended in a future study to further scenes from Hexagon, Corona, MSS, TM, ETM+, OLI, and ASTER.

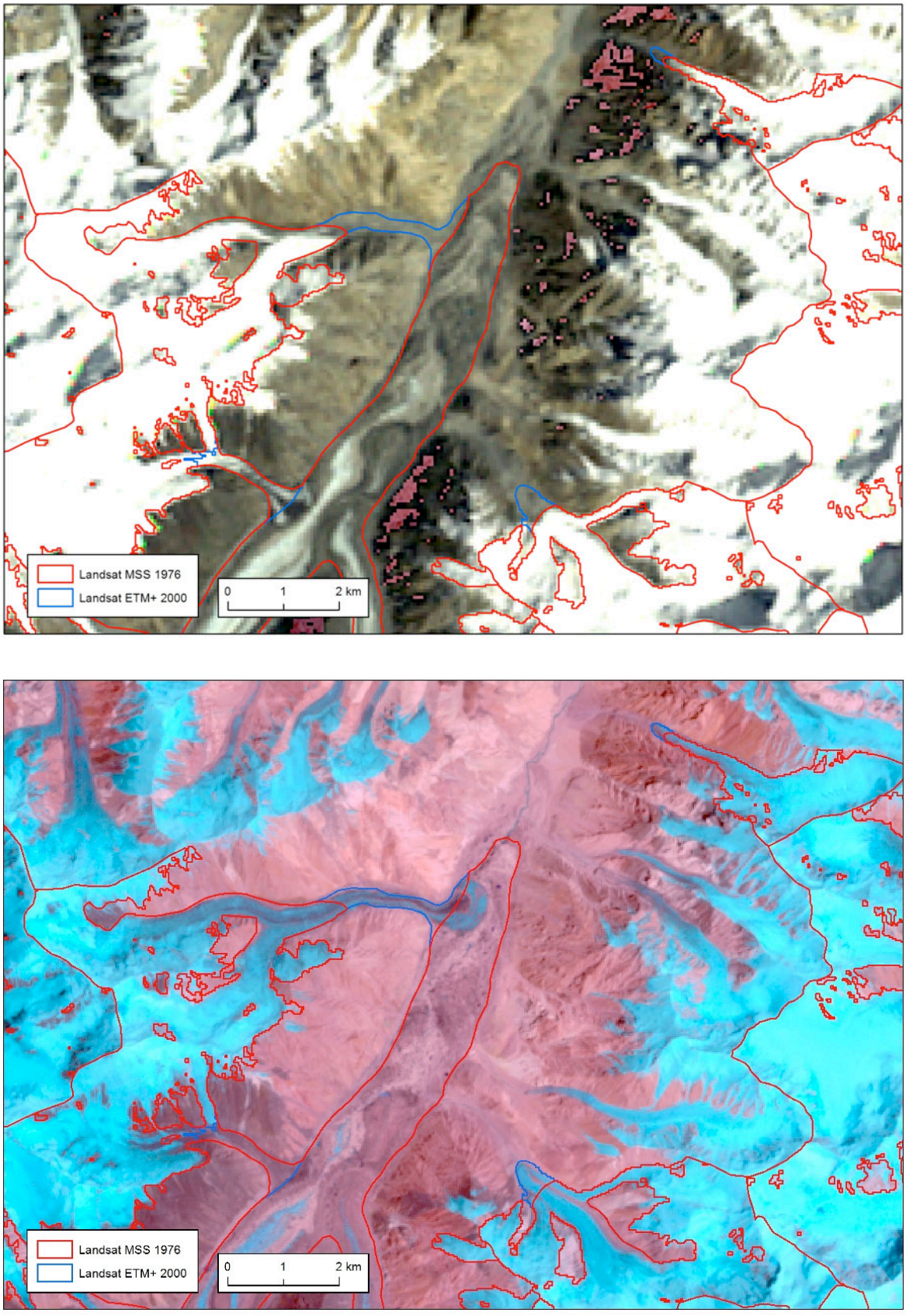

Fig. 1: MSS (top) and ETM+ (bottom) scene for the Sarpo Laggo Basin with glacier outlines from both points in time (1976: red, 2000: blue).

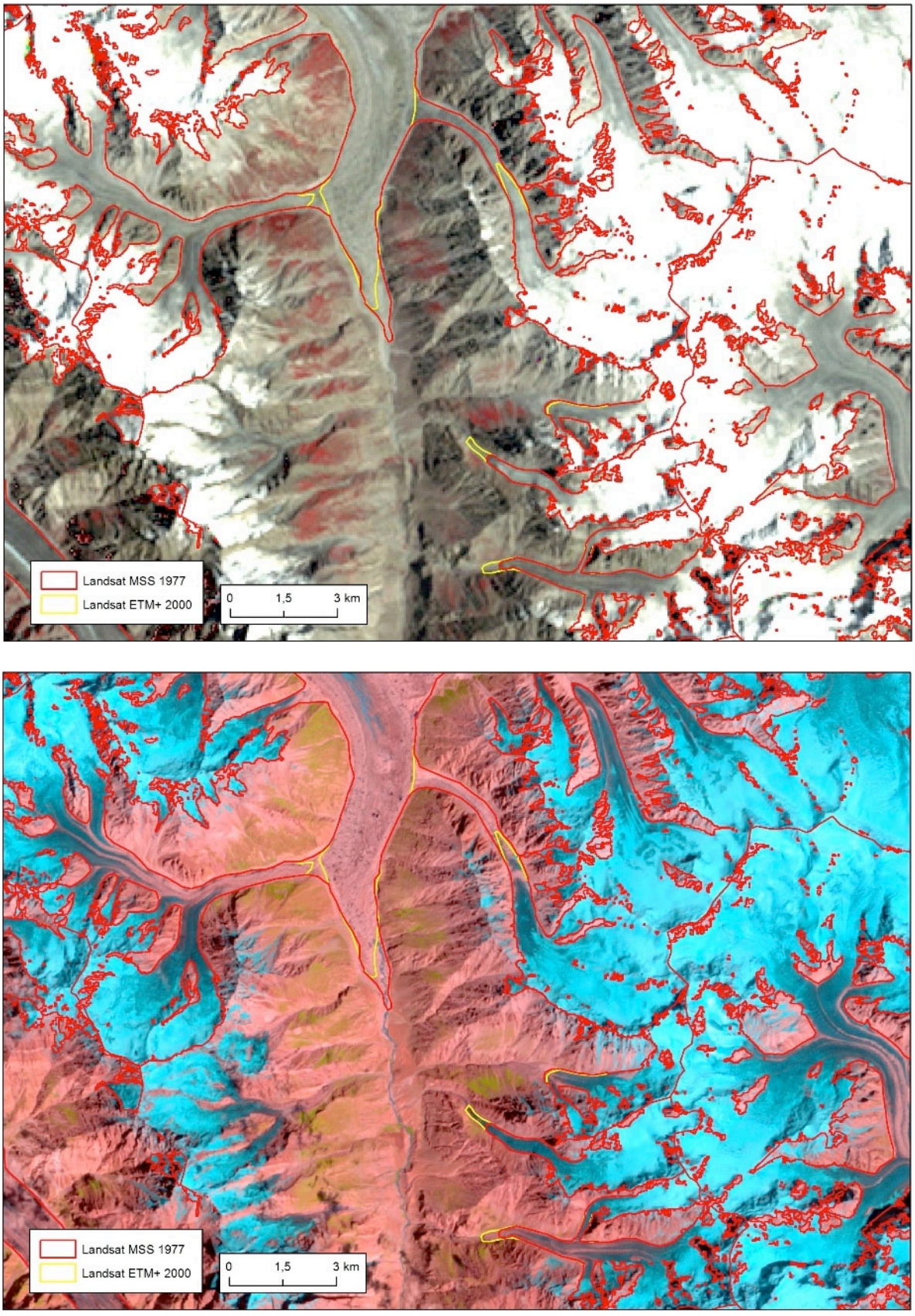

Fig. 2: MSS (top) and ETM+ (bottom) scene for the lower Panmah Basin with glacier outlines from both points in time (1977: red, 2000: yellow).

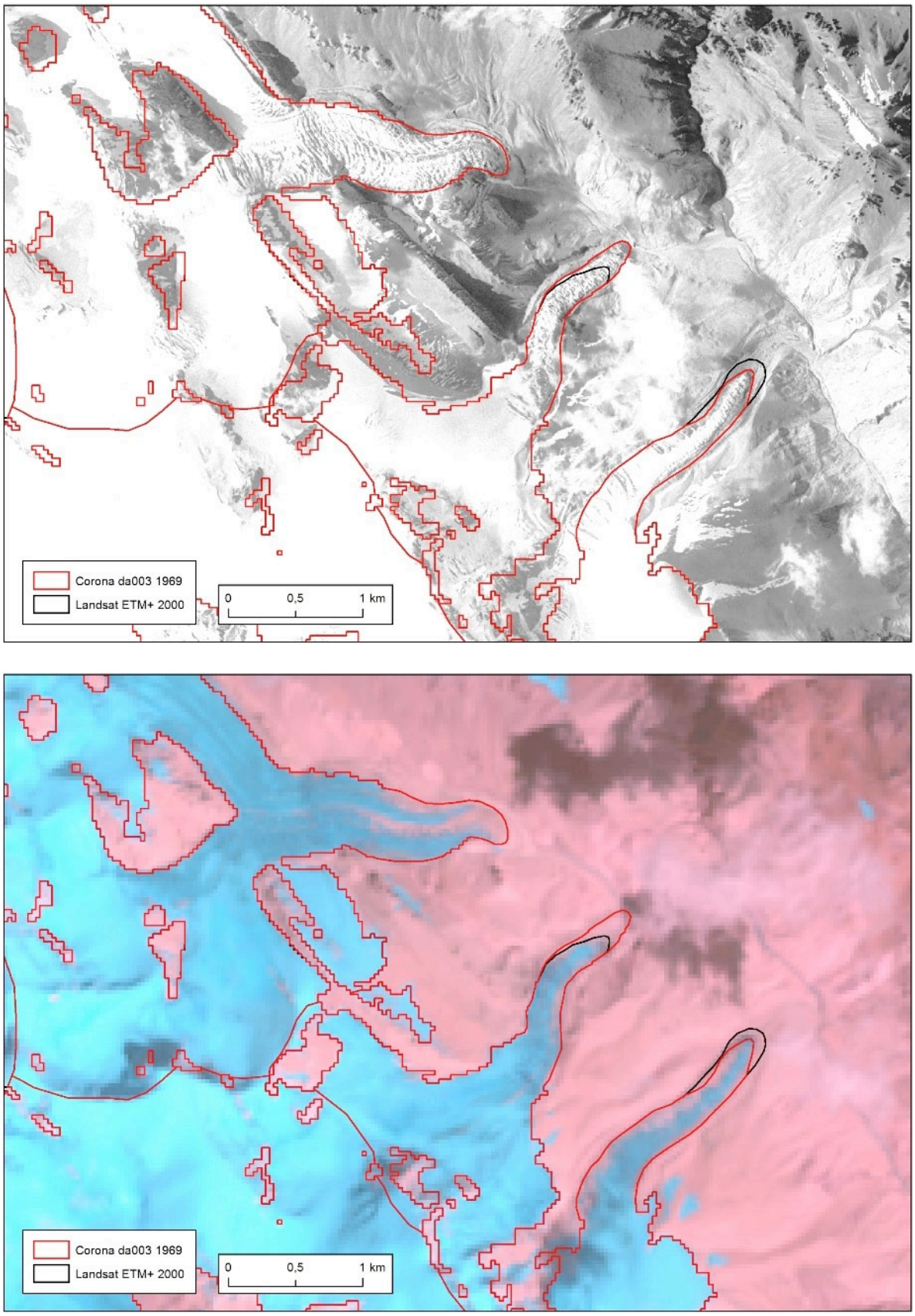

Fig. 3: Corona (top) and ETM+ (bottom) scene just north of Shaksgam Valley with glacier outlines from both points in time (1969: red, 2000: black).

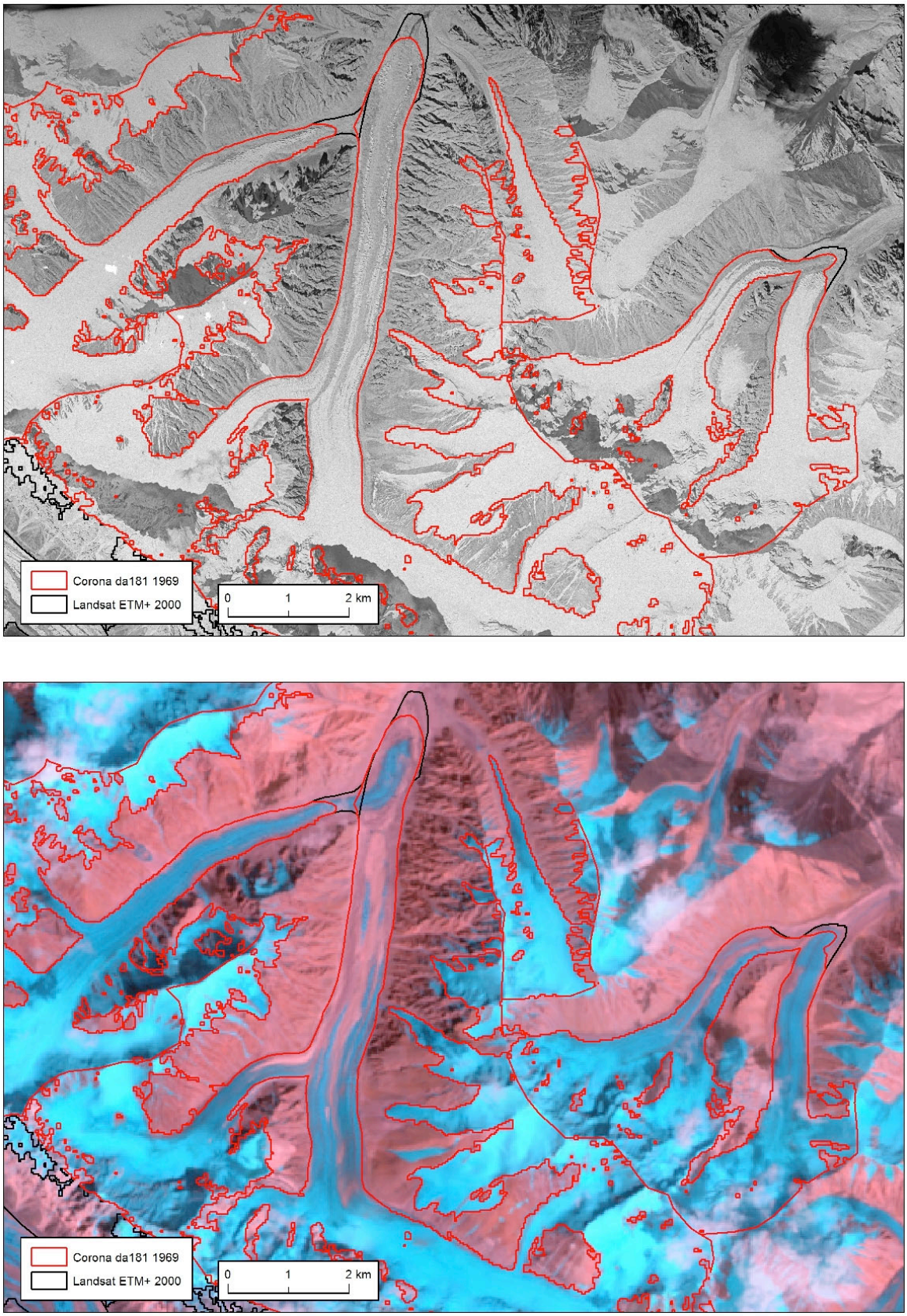

Fig. 4: Corona (top) and ETM+ (bottom) scene for the Shaksgam Valley with glacier outlines from both points in time (1969: red, 2000: black).

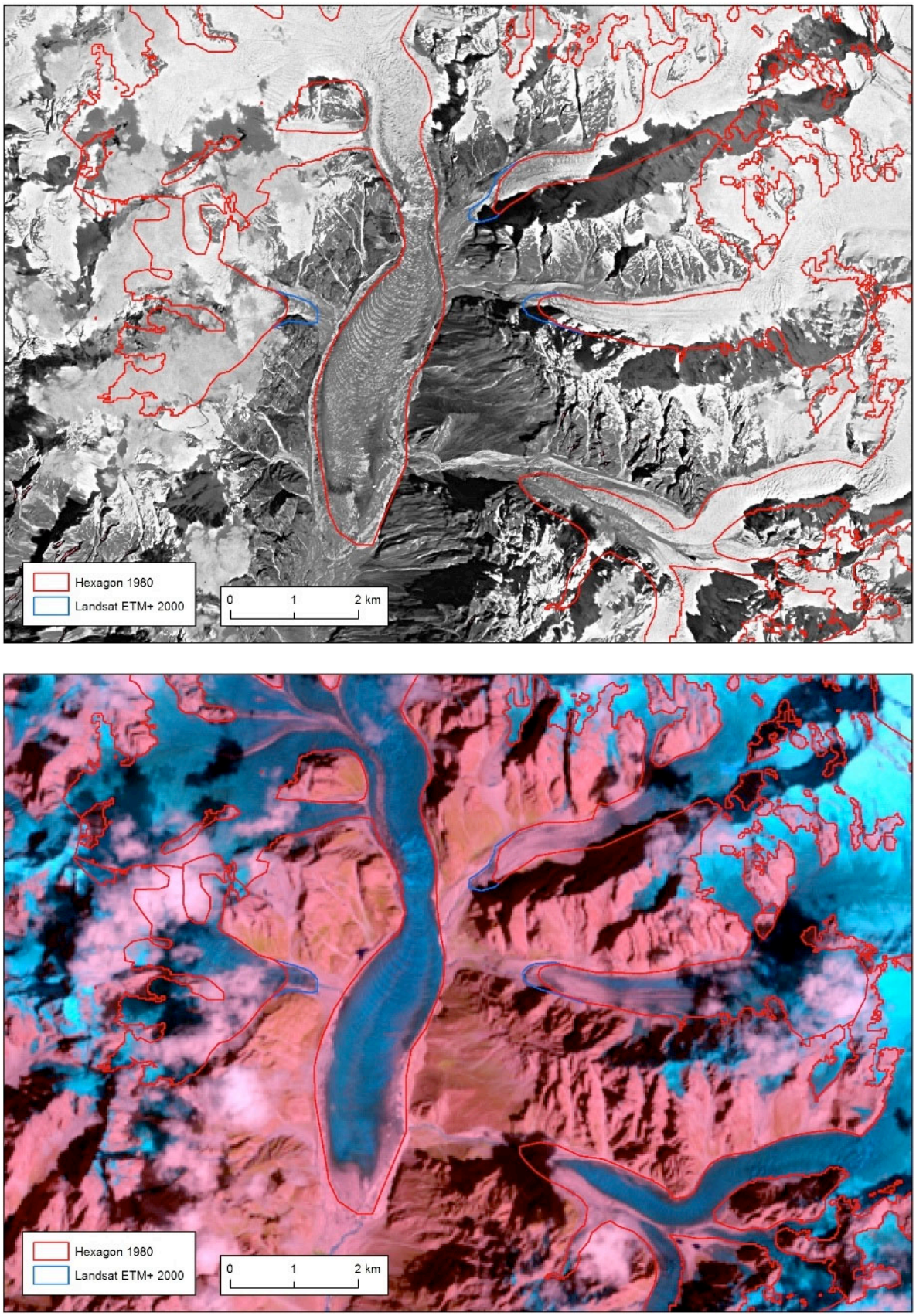

Fig. 5: Hexagon (top) and ETM+ (bottom) scene for the Khore-Kondo glacier (west of Siachen glacier) with outlines from both points in time (1980: red, 2000: blue).

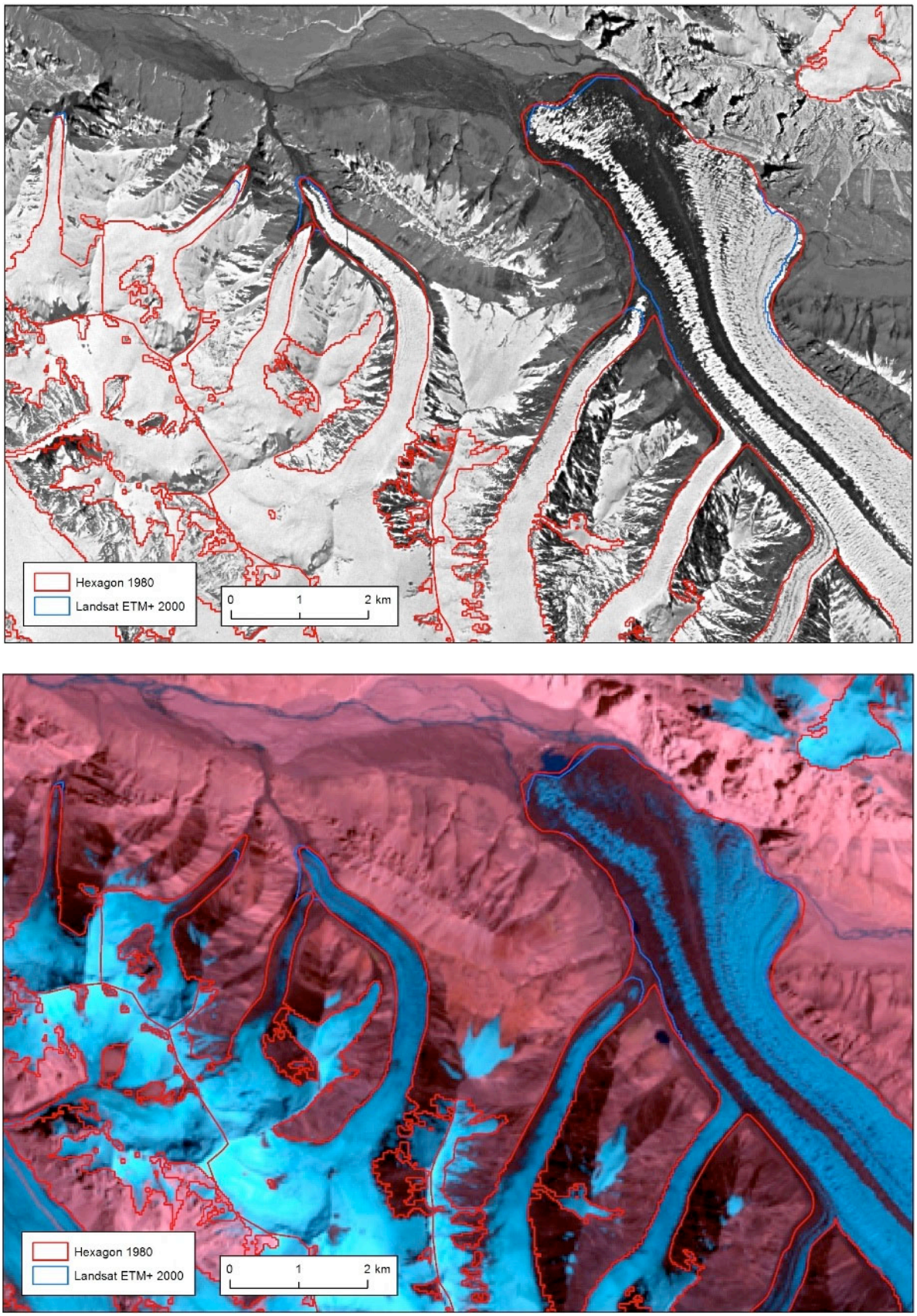

Fig. 6: Hexagon (top) and ETM+ (bottom) scene for the Shaksgam Valley with glacier outlines from both points in time (1980: red, 2000: blue).

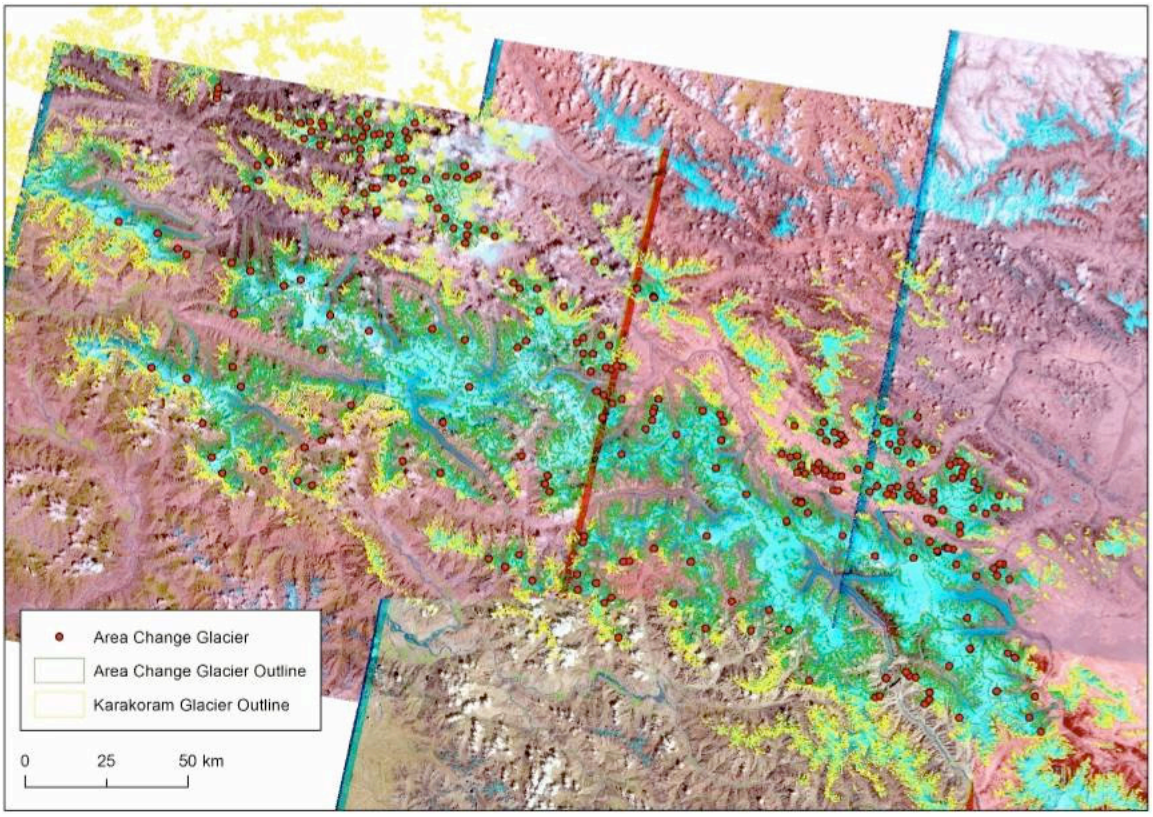

Fig. 7: Overview map showing the glaciers for which change assessment has been performed.

2.3 Uncertainties

The estimation of uncertainty follows the suggestions in UCRv2 (Glaciers_cci 2014), summing up the uncertainties from both points in time (master image + historic image), according to the principles of error propagation. The master image uncertainty is estimated as ±½ pixel, corresponding to ~15 m. Uncertainties for the historic images depend on the spatial resolution, in which they have been processed, which is ~10 m for Corona and Hexagon and ~60 m for MSS. In case of additional complications (low contrast, seasonal snow, debris coverage, poor geometric quality) the uncertainty has been raised from half a pixel to one pixel, which applies to the MSS-scene from 1973 and all Corona and Hexagon scenes (due to the often poor geometric quality). This led to the following horizontal uncertainties: 25 m (15 + 10) for Corona/Hexagon, 75 m for MSS 1973 (15 + 60) and 45 m (15 + 30) for MSS 1976 and 1977.

Because the corrections were only performed in the terminus regions, also the uncertainties are only found here. We used the area change between the master and the historic image („A“), created a buffer around it („A+B“) and calculated the difference (|„A+B“-„A“|). In case this difference was larger than the area change (“A”) itself – i.e. the uncertainty is exceeding the change – the area change was considered insignificant and therefore set to zero. In the case the difference was smaller, the glaciers have been classified according to the intensity of change: advancing (positive change >0.01 km²), receding (negative change >0.01 km²), and stationary. This type of separation has been chosen because absolute values of area change cannot be given when only terminus changes are investigated (i.e. changes in other parts of the glacier are neglected).

2.4 Results

A glacier was considered stationary, if its change was within ±0.01 km² or the uncertainty is exceeding the change as described above. In total, 394 comparison values for 251 different glaciers have been obtained. Of these, 161 glaciers have two comparison periods, 51 glaciers have three, 25 have three and 14 four periods. Table 1 shows the results per considered satellite scene. As an example: in the 1976 MSS scene 79 glaciers have been investigated, 57 of which have shown a change in area, but only 23 have changed significantly; twelve out of these 23 have advanced while eleven have receded; the rest (56) has remained stationary.

The glaciers with multiple assessment periods show a consistent behaviour through time, i.e. they never change their trend. To get a more comprehensive picture for the entire region, the multitemporal information was assembled by prioritising advance/retreat over stationary cases. For example, a glacier with stationary behaviour in one image pair but advancing in another one got the label "advancing". In total, this sums up to 191 out of 251 glaciers being stationary, 33 receding and 27 advancing (Fig. 8). The observed maximum changes are -2.4 km² and +1.4 km² for two glaciers between 72/76/77 and 2000. Summing up the maximum and minimum values for all advancing and receding glaciers, the area increase is 7.6 km², while the loss is 14.5 km².

For comparison with Fig. 8 (covering about the same region) Fig. 9 shows a classification of glaciers by Rankl et al. (2014) that is mostly based on the analysis of satellite images from the years 2000-2012. That study also identified surge-type glaciers from a range of criteria. On a more rough scale it seems that in particular the surge cluster north of Biafo and Baltoro glaciers (marked Bi and Bt in Fig. 9) have started a surge phase after 2000 and retreated before. But in more detail, the changes are rather complex and require further analysis.

We conclude that the processing and analysis of MSS / Corona / Hexagon data could be worth the effort (if good quality data exist), but it has to be checked on a case-by-case basis and is depending on what is available from other sources (e.g. from historic topographic maps). A more in-depth analysis of the periodicity of surge cycles would certainly be interesting.

	da003_69	da004_69	da181_69	MSS72	MSS76	MSS77	hex80	Total
N gl ch	14	12	5	40	57	90	37	255
N gl sig	2	4	4	5	23	27	19	84
N gl stat	14	13	2	8	22	32	48	139
N gl adv	2	3	5	14	28	30	12	94
N gl adv sig	0	3	4	1	12	11	7	38
N gl ret	12	9	0	25	29	59	24	158
N gl ret sig	2	1	0	4	11	16	12	46
N gl total	28	25	7	48	79	122	85	394

Table 1: Glacier change statistics for the selected scenes. Abbreviations: N = Number; gl = glacier; ch = changing; stat = stationary; adv = advancing; ret = retreating; sig = significantly.

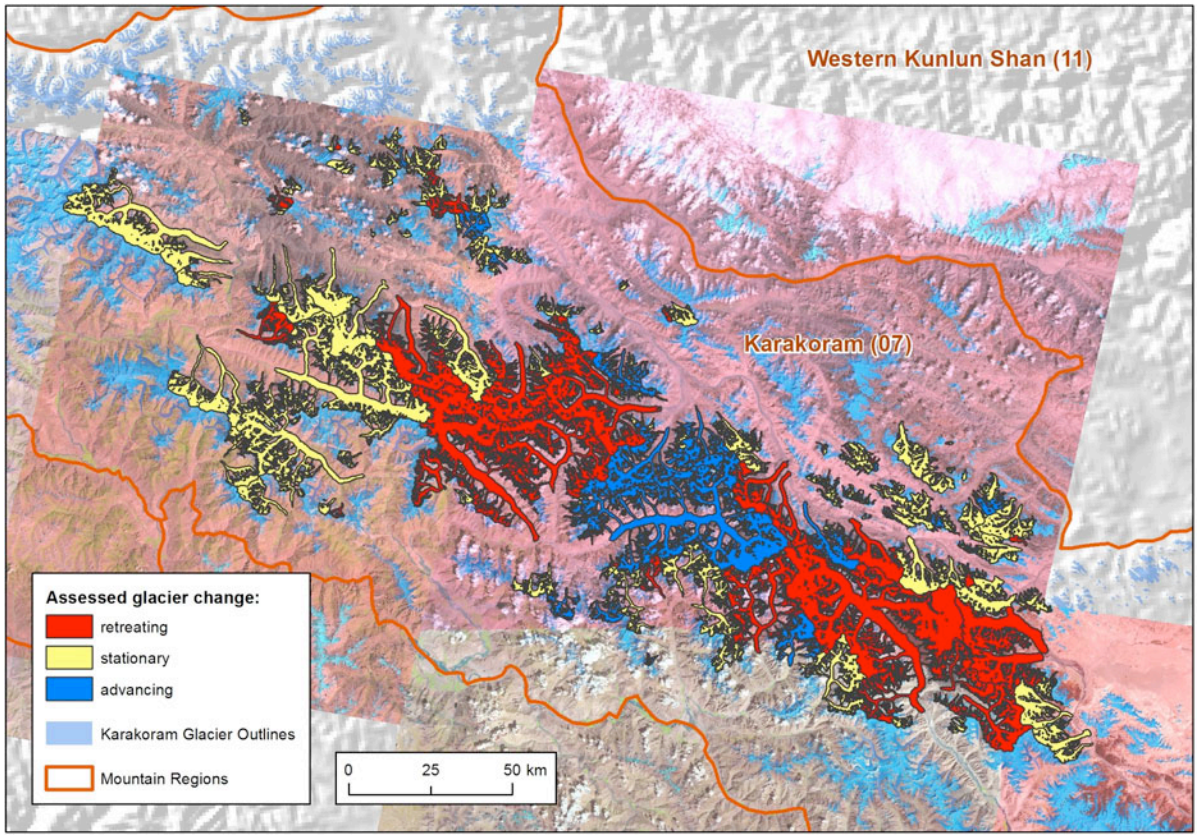

Fig. 8: Overview of the area changes for 251 glaciers over the period 1970s/80s to 2000, classified into three classes.

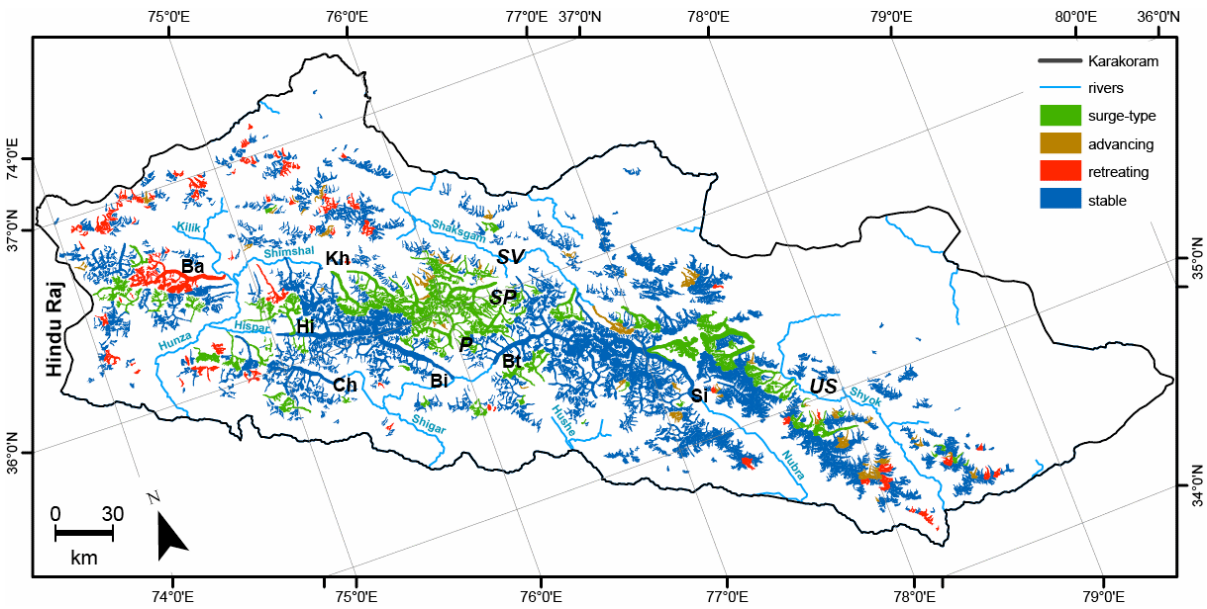

Fig. 9: Glacier classification in the Karakoram according to Fig. 3 of Rankl et al. (2014). The classification is mostly based on observations for the period 2000-2012.

3. Elevation changes using the new glacier outlines

3.1 Background

Computing glacier elevation trends from ICESat elevations over 2003-2009 requires separation of footprints over glaciers from other footprints (Kääb et al. 2012). There are two principle ways to classify ICESat footprints: (1) overlaying the footprint locations over satellite imagery and classifying them manually, or (2) use or prepare a glacier inventory or other land cover classification to intersect the footprints with. In both cases, the quality of the ICESat-derived elevation trends depends on the quality of these classifications. Too many non-glacier (land) points could for instance weaken a negative or positive glacier elevation trend. Too many glacier points in the land sample could bias the land trend, which should approach zero. The impact of too many glacier points classified into the land class can vary, depending on the type of misclassified glacier points. If specifically glacier points with comparable little elevation change are misclassified, the estimate of a negative glacier trend will be more negative, and vice-versa. Also, land points are not necessarily stable as they can, for instance, actually fall on glacier lakes. In summary, misclassifications of glacier points (either land points falsely classified as glacier, or actual glacier points not classified as glaciers) can have all kinds of impacts on glacier elevation trends; increase trends, weaken trends, or even cancel out and have thus little influence. Figure 10 provides an overview of the new Glacier_cci inventories (CCI) for which results were compared against those from the previous RGI (v3.0).

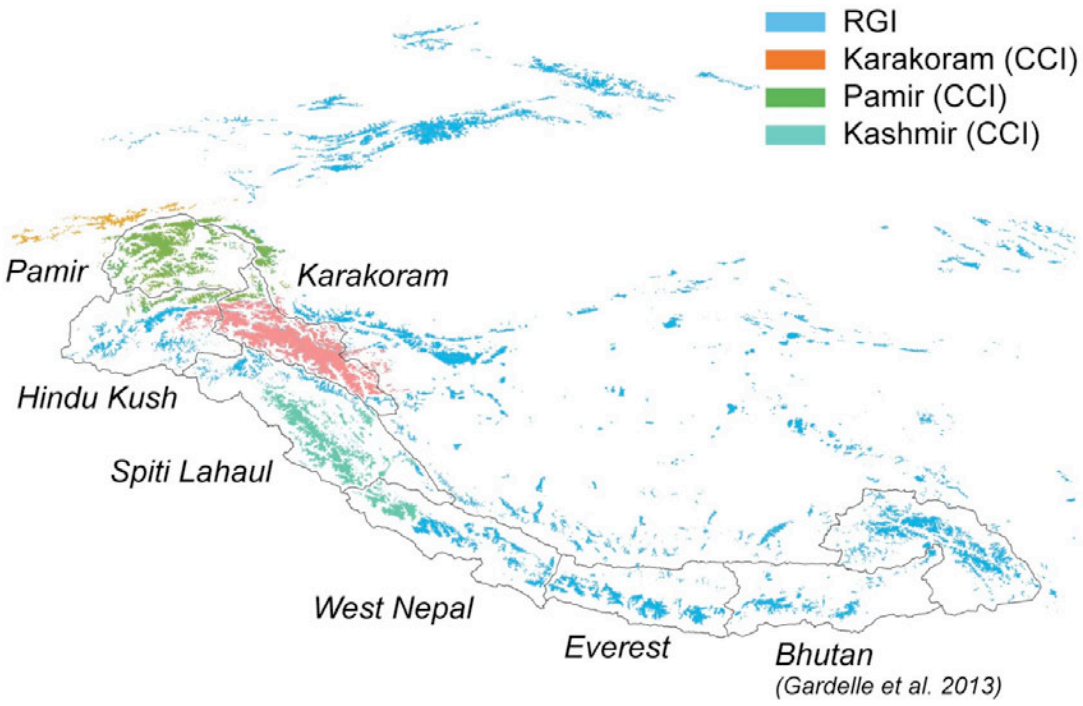

Fig. 10. Overview of glacier inventories used in this study and zones referred to in the text and Table 2. The Randolph Glacier Inventory (RGI, blue) and Glaciers_cci (CCI) inventories from the Karakoram, Pamir and Kashmir are superimposed in different colours. Outlines and names refer to zones by Gardelle et al. (2013).

In this sensitivity study, we compare ICESat-derived glacier elevation trends over the Pamir-Karakoram-Himalaya region based on manually classified footprints and those intersected with different glacier inventories. The ICESat methods follow Kääb et al. (2012) and use autumn data only, unless stated otherwise. For the manual footprint classifications, Landsat 7 or 8 data with minimum snow cover between 2000 and 2013 have been loaded in a GIS and un-classified ICESat footprints overlain. Then all glacier areas were systematically visited, and ICESat footprints over glaciers and lakes selected separately with a polygon selection tool and given unique class codes (Figs. 11 and 12). For Karakoram and Himalaya, in addition footprints over debris-covered glacier parts were selected and given an own class code. This procedure was performed by Glaciers_cci staff at GUIO. The classifications were performed before Glacier_cci outlines became available, so that the comparison between both represents an independent validation. The accuracy of the manual classifications turned out to be very similar to Glaciers_cci outlines (Fig. 12). In the following we discuss the different data sets.

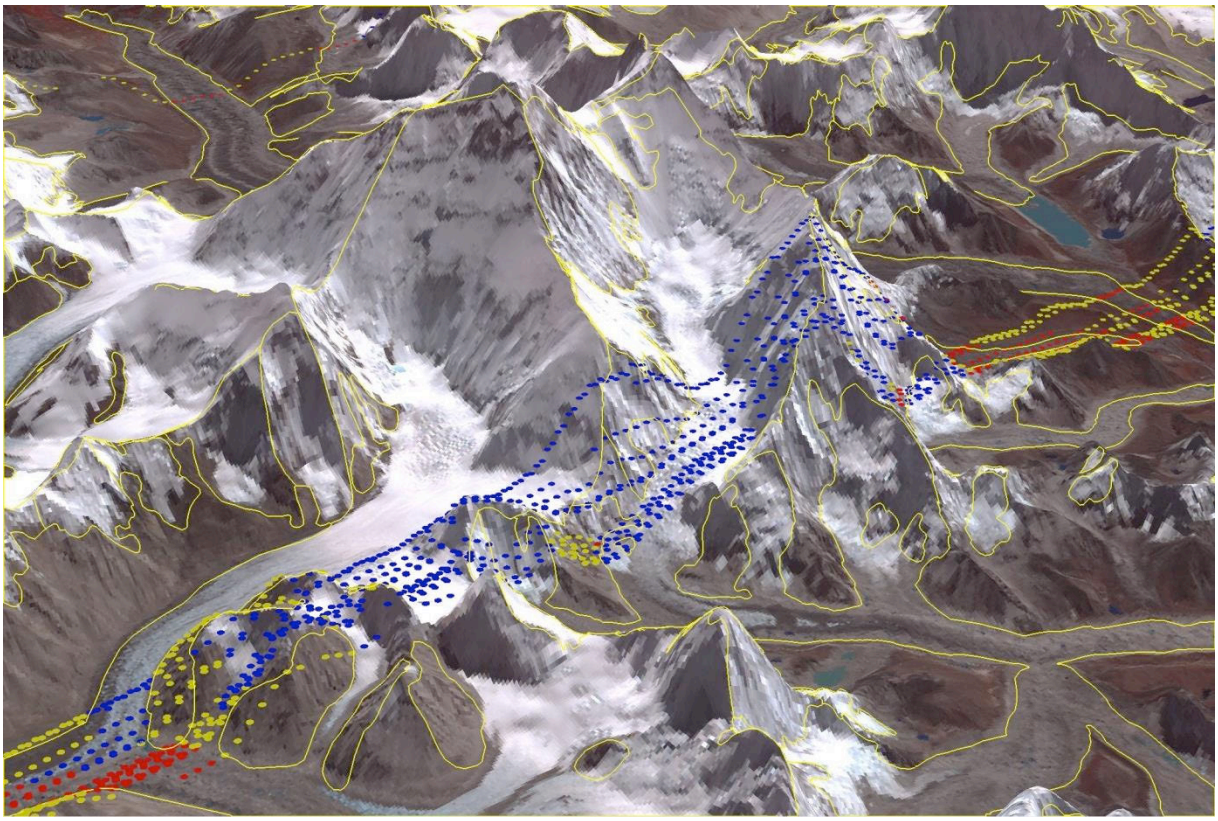

Fig. 11: Oblique view on Mt. Everest, Nepal, with the background image from ASTER draped over the DEM. Yellow glacier outlines are from the RGI. ICESat points are footprints manually classified; yellow: land, blue: ice/snow; red: debris-covered ice. Classifications are taken from Kääb et al. (2012). In the section shown, the RGI is of a useful quality and fits quite well to the footprint classifications.

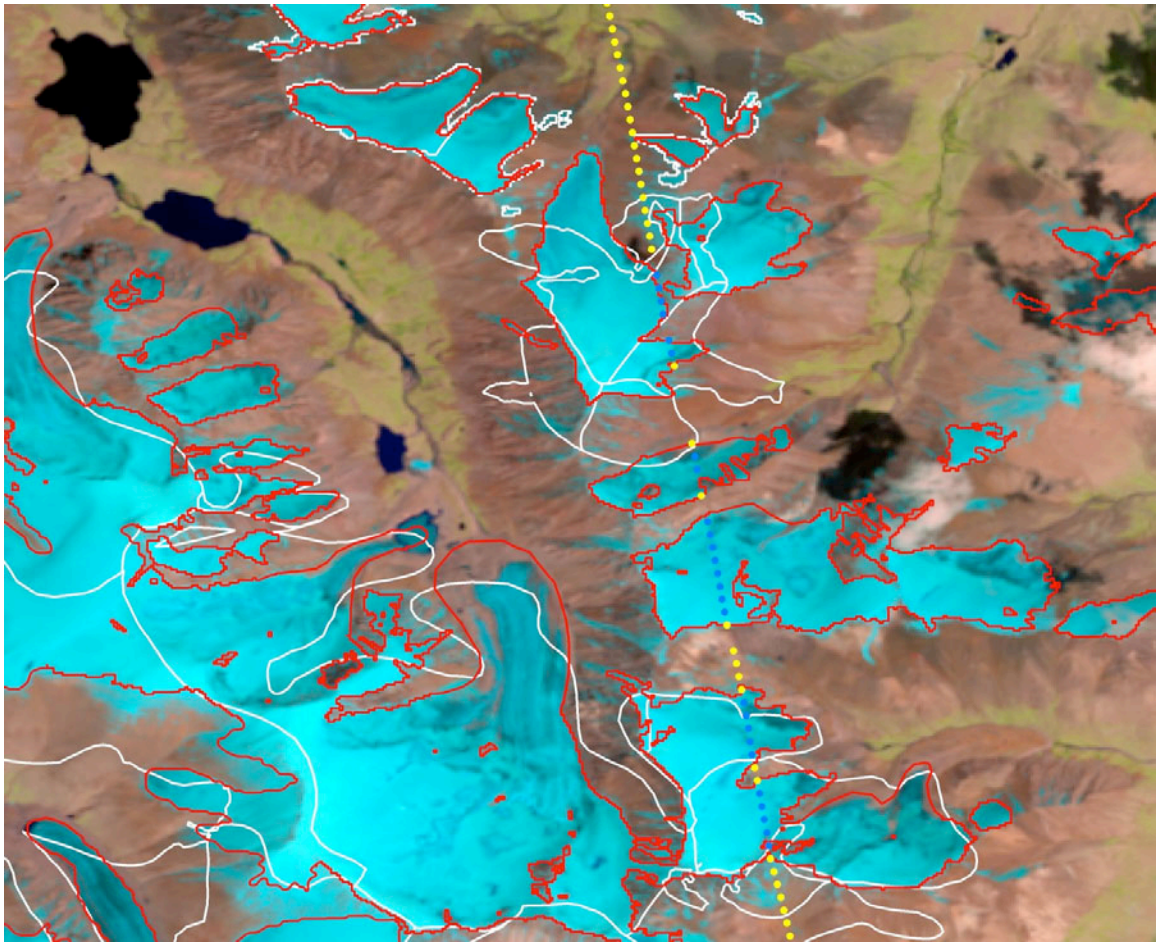

Fig. 12: Example of glacier outlines and ICESat footprint classifications in the eastern Pamir. The RGI (white outlines), Glaciers_cci outlines (red), manual ICESat footprint classifications (yellow: land; blue: ice). This section shows an area with poor RGI quality.

3.2 Study regions

Karakoram

This test refers to the region covered by the Glaciers_cci inventory derived in this option. Elevation trends based on manually classified footprints and based on the new Glaciers_cci inventory are almost identical (Table 2). Trends based on the existing RGI are slightly less negative. Even if the CCI outlines are visually clearly better (see Fig. 12) than the RGI ones, the impact on ICESat elevation trends is small in total.

Pamir

This test refers to the region covered by the new Glaciers_cci inventory. Trends of all three classifications (manual, Glaciers_cci outlines, RGI outlines) are identical (Table 2). Even if the Glaciers_cci outlines are visually clearly better than the RGI ones (see Fig. 12), the impact on ICESat elevation trends is small overall.

Kashmir

This test refers to the region covered by the GlobGlacier / Glaciers_cci inventory. Here, no RGI data existed before the GlobGlacier / Glaciers_cci inventory. ICESat glacier trends based

on manual classification and the inventory are almost identical, which is no surprise given the high quality of GlobGlacier/Glaciers_cci inventories and also found for the other test cases.

Entire region

We also compare trends from manually classified footprints against those classified using the RGI for the entire region from Pamir to Bhutan (Table 2). The zones used are those from Gardelle et al. (2013). The differences are smallest for Karakoram, Pamir and Bhutan, and largest for West Nepal and Everest, up to 50%. These areas contain monsoon-type glaciers that may be covered and surrounded by significant amounts of snow also in the ablation or dry season. As a consequence manual and automated classifications are complicated by the interpretation of glacier areas versus non-glacier snow cover. Different glacier interpretation principles in the two data sets could also have impacted on the different elevation trends. We also compare elevation trends for windows of 2 × 2 degree size. Here, the average absolute deviation between both trends is ~50%, with a number of cells showing deviations on the order of 100%.

3.3 Results

In most tests, the difference between ICESat-derived glacier elevation trends based on manually classified footprints and those based on glacier inventories are not drastic, sometimes even very small (Table 2). In some cases the differences are, however, up to 50% for entire regions. The differences get bigger for smaller units, e.g. geographic cells of 2 × 2 degree, where the average deviation is around 50%. Roughly, the effects from footprint classifications tend to cancel each other out over larger zones, at least for the Pamir-Karakoram-Himalayas region investigated here, even if they are considerable locally. It is also important to note that such potential deviations from footprint misclassifications are typically not contained in error budgets, so that the deviations found here would have to be added to the uncertainties.

It is also important to note that such potential deviations from footprint misclassifications are typically not contained in error budgets, so that the deviations found here would have to be added to the uncertainties. A formal incorporation of such errors is not straight forward as the underlaying missclassifications can have various effects on derived trends (see section 3.1), from increasing or weakening trends, to even cancelling out. A related sound methodology will have to be explored in Glaciers_cci Phase 2. In conclusion, it seems feasible to:

- Check off-glacier trends for their proximity to zero. Misclassifications will in many cases deviate the off-glacier trend from zero when restricted to footprints close to glaciers.
- Select some test areas where manual footprint classifications are prepared (if not done anyway) and compared to glacier outlines. From the number and kind of differences an error estimate can be produced under assumptions of typical glacier elevation changes.
- Perform bootstrapping or Monte Carlo simulations to randomly misclassify footprints and assess the effect on derived trends.

A more automated assignment of footprint classifications would become possible if glacier inventories would separately identify (as a polygon) the debris-covered parts. A related study should be performed in Phase 2 of Glaciers_cci.

Zone	Glacier classification	Elevation trend ± standard error	Footprint # land / glacier
Karakoram	Manual	-0.13 ± 0.04 m/yr	18154 / 17319
	CCI	-0.14 ± 0.04 m/yr	19728 / 15745
	RGI	-0.09 ± 0.04 m/yr	21630 / 13843
Pamir	Manual	-0.47 ± 0.07 m/yr	11558 / 6112
	CCI	-0.47 ± 0.07 m/yr	11664 / 6006
	RGI	-0.47 ± 0.07 m/yr	11880 / 5790
Kashmir	Manual	-0.53 ± 0.05 m/yr	26778 / 9614
	CCI/GlobGlacier	-0.54 ± 0.05 m/yr	27654 / 8738
Zones from Gardelle et al. (2013)			
Everest	Manual	-0.37 ± 0.09 m/yr	8623 / 4595
	RGI	-0.57 ± 0.11 m/yr	9909 / 3309
Bhutan	Manual	-0.89 ± 0.13 m/yr	5555 / 2222
	RGI	-0.91 ± 0.14 m/yr	5900 / 1877
West Nepal	Manual	-0.43 ± 0.08 m/yr	12797 / 4893
	RGI	-0.54 ± 0.08 m/yr	13513 / 4177
Karakoram	Manual	-0.10 ± 0.04 m/yr	12679 / 16027
	RGI	-0.08 ± 0.04 m/yr	16087 / 12619
Spiti Lahaul	Manual	-0.49 ± 0.05 m/yr	24842 / 8407
	RGI	-0.46 ± 0.05 m/yr	25632 / 7617
Pamir	Manual	-0.48 ± 0.08 m/yr	6882 / 4364
	RGI	-0.47 ± 0.08 m/yr	7055 / 4191
Hindu Kush	Manual	-0.49 ± 0.08 m/yr	9286 / 3718
	RGI	-0.40 ± 0.09 m/yr	10127 / 2877
Entire region	Manual	-0.36 ± 0.03 m/yr	80664 / 44226
	RGI	-0.38 ± 0.03 m/yr	88223 / 36667

Table 2: Comparison of elevation trends 2003-2009 using different footprint classifications.

References

Bhambri, R., Bolch, T., Kawishwar, P., Dobhal, D., Srivastava, D. and Pratap, B. (2013): Heterogeneity in glacier response in the Shyok valley, northeast Karakoram. The Cryosphere, 7, 1384-1398.

Copland, L., Sylvestre, T., Bishop, M., Shroder, J., Seong, Y., Owen, L., Bush, A., and Kamp, U. (2011): Expanded and recently increased glacier surging in the Karakoram, Arctic Antarctic and Alpine Research, 43, 503-516.

Gardelle, J., Berthier E., Arnaud Y. and Kääb A. (2013): Region-wide glacier mass balances over the Pamir-Karakoram-Himalaya during 1999–2011. The Cryosphere, 7, 1263-1286.

Gardner, A. S., Moholdt, G., Cogley, J. G., Wouters, B., Arendt, A.A., Wahr, J., Berthier, E., Pfeffer, T.W., Kaser, G., Hock, R., Ligtenberg, S.R.M., Bolch, T., Sharp, M.J., Hagen, J. O., van den Broeke, M. R. and Paul, F.: (2013): A reconciled estimate of glacier contributions to sea-level rise: 2003 to 2009. Science, 340, 852-857.

Glaciers_cci (2014): Uncertainty Characterization Report version 3 (UCRv3). Prepared by the Glaciers_cci consortium, 32 pp.

Hewitt, K. (2007): Tributary glacier surges: an exceptional concentration at Panmah Glacier, Karakoram Himalaya. Journal of Glaciology, 53, 181-188.

Kääb, A., Berthier, E., Nuth, C., Gardelle, J. and Arnaud, Y. (2012): Contrasting patterns of early twenty-first-century glacier mass change in the Himalayas. Nature, 488 (7412), 495-498.

Pieczonka, T., Bolch, T., Wei, J. and Liu, S. (2013): Heterogeneous mass loss of glaciers in the Aksu-Tarim Catchment (Central Tien Shan) revealed by 1976 KH-9 Hexagon and 2009 SPOT-5 stereo imagery. Remote Sensing of Environment, 130, 233-244.

Rankl, M., Kienholz, C. and Braun, M. (2014): Glacier changes in the Karakoram region mapped by multimission satellite imagery. The Cryosphere, 8, 977-989.

Abbreviations

ASTER	Advanced Thermal Emission and Reflection radiometer
ETM+	Enhanced Thematic Mapper plus
GCP	Ground Control Point
GIDP	Glacier Inventory Data Package
GUIO	Department of Geosciences, University of Oslo
ICESat	Ice, Cloud, and Elevation Satellite
MSS	MultiSpectral Scanner
OLI	Operational Land Imager
RGI	Randolph Glacier Inventory
SAR	Synthetic Aperture Radar
SRTM	Shuttle Radar Topography Mission
TM	Thematic Mapper